RNA-binding protein MBNL1 regulates tumor growth, chemosensitivity and antitumor immunity in lung adenocarcinoma by controlling the expression of tumor suppressor RNF125

YUBO YAN, XIANGLONG KONG, XIANGYUAN JIN, JIANLONG BU, BOXIONG NI, ZUQIN RAO, JUNNAN GUO and SHIDONG XU

Department of Thoracic Surgery, Harbin Medical University Cancer Hospital, Harbin, Heilongjiang 150000, P.R. China

Received October 23, 2024; Accepted April 1, 2025

DOI: 10.3892/or.2025.8907

Abstract. Ring finger protein 125 (RNF125), a ubiquitin E3 ligase, has been reported to act as a tumor suppressor in several cancers, but its precise function in lung adenocarcinoma (LUAD) has not been elucidated. In the present study, through bioinformatics analysis and immunohistochemistry in LUAD and non-cancerous samples, it was demonstrated that RNF125 was significantly downregulated in lung cancer. Low levels of RNF125 expression were associated with metastatic status, advanced tumor stage and poor overall survival in LUAD. The results of gain- and loss-of-function experiments demonstrated that RNF125 inhibited proliferation, colony formation, migration and invasion of LUAD cells. In addition, RNF125 increased the sensitivity of LUAD cells to cisplatin. Mechanistically, RNF125 interacted with programmed cell death ligand 1 (PD-L1) and reduced PD-L1 expression levels in LUAD cells. Furthermore, IL-2 secretion by Jurkat T cells was significantly suppressed when co-cultured with RNF125-silenced LUAD cells. NK-92 cell lysis of RNF125-silenced LUAD cells was also weaker compared with that of control LUAD cells, suggesting that RNF125 knockdown enhanced the immune evasion ability of LUAD cells. Notably, the results of the present study identified that the RNA-binding protein muscleblind-like 1 (MBNL1) is the upstream regulator of RNF125 in LUAD. MBNL1 increased the stability of the RNF125 transcript in LUAD cells and knockdown of RNF125 reversed the antitumor effect of MBNL1 on LUAD cells. In conclusion, the present study demonstrated the tumor suppressor role of RNF125 in LUAD and implicated MBNL1 as an upstream regulator of RNF125 in LUAD. These findings contributed to an improved understanding of the molecular features of LUAD progression.

Correspondence to: Dr Shidong Xu, Department of Thoracic Surgery, Harbin Medical University Cancer Hospital, 150 Haping Road, Nangang, Harbin, Heilongjiang 150000, P.R. China
E-mail: xushidong0106@163.com

Abbreviations: Co-IP, co-immunoprecipitation; IHC, immunohistochemical; LC, lung cancer; LUAD, lung adenocarcinoma; MBNL1, muscleblind-like 1; *p*NA, *p*-nitroaniline; PARP, poly ADP-ribose polymerase; PD-L1, programmed cell death ligand 1; RBP, RNA-binding protein; RIP, RNA immunoprecipitation; RNF125, ring finger protein 125

Key words: cisplatin, immune escape, lung adenocarcinoma, muscleblind-like 1, programmed cell death ligand 1, ring finger protein 125

Introduction

Lung cancer (LC) was the most frequently diagnosed cancer and was responsible for the largest proportion of all cancer-related deaths worldwide in 2022 (1-3). Lung adenocarcinoma (LUAD) is the most common type of LC, comprising almost one-half of all LC cases globally (4-6). LUAD is typically diagnosed at an advanced stage and is highly resistant to conventional radiotherapy and chemotherapy (4,7,8). Therefore, it is important to search for potential therapeutic targets.

Ubiquitination is a highly conserved post-translational modification in eukaryotes that is catalyzed by an enzymatic cascade involving the sequential action of E1, E2 and E3 enzymes (9). In previous decades, the role of E3 ubiquitin ligase in regulating numerous cellular processes has attracted increasing interest due to its essential function in determining the specificity and fate of target proteins. Ring finger protein 125 (RNF125; also termed TRAC-1) functions as a ubiquitin E3 ligase in lymphoid tissues that positively regulates T cell activation (10,11). Previous studies have shown that RNF125 can suppress the progression of several cancers, including hepatocellular carcinoma, head and neck squamous cell carcinoma and melanoma (12-15). However, the functional role of RNF125 in LUAD is largely unknown.

Programmed cell death ligand 1 (PD-L1) is a transmembrane protein that is regarded as a co-suppressor of the immune response (16). PD-L1 also serves a pro-oncogenic role in various malignancies, including LC, by attenuating the host immune response to tumor cells (17). Knockdown of GFAT1, a positive regulator upstream of PD-L1, has been shown to significantly enhance T cell activation and NK cell killing of LC cells (18). A previous study showed that high PD-L1

expression was associated with poor prognosis in patients with LUAD and correlated with immune-related pathways (19). A previous study reported that RNF125 promoted K48-linked polyubiquitination of PD-L1 and mediated its degradation (20). Therefore, it could be hypothesized that RNF125 enhances tumor immunity and reduces PD-L1 expression levels in LUAD.

Muscleblind-like 1 (MBNL1), an RNA-binding protein (RBP), increases the stability of downstream gene transcripts by binding to their 3' untranslated region (UTR), resulting in the upregulation of gene expression levels (21,22). A number of studies have shown that MBNL1 inhibits cancer cell proliferation, migration and invasion, and suppresses tumor progression in breast cancer, gastric cancer and glioblastoma (21,23,24). Additionally, MBNL1 expression is reduced in LC tissues and is associated with poor prognosis in patients (23). TIMER2.0 database (http://timer.cistrome.org/) analysis revealed that MBNL1 was positively correlated with RNF125 expression levels in LUAD tissues (25). Meanwhile, the RBPDB database (http://rbpdb.ccbr.utoronto.ca/) predicted that the RNF125 transcript 3'UTR has putative MBNL1-binding sites (26). Whether MBNL1 upregulates RNF125 expression levels by increasing the stability of RNF125 transcripts needs to be further clarified.

The present study aimed to investigate the role of RNF125 in LUAD progression, focusing on its effects on tumor growth, chemosensitivity and antitumor immunity, as well as its upstream and downstream molecular mechanisms.

Materials and methods

Bioinformatics. Gene Expression Omnibus Series datasets GSE75037 (https://www.ncbi.nlm.nih.gov/geo/query/acc.cgi?acc=gse75037) (27), GSE31210 (https://www.ncbi.nlm.nih.gov/geo/query/acc.cgi?acc=GSE31210) (28,29) and GSE116959 (https://www.ncbi.nlm.nih.gov/geo/query/acc.cgi?acc=GSE116959) (30) containing LUAD and corresponding non-cancer samples were retrieved from the National Institutes of Health Gene Expression Omnibus dataset database (https://www.ncbi.nlm.nih.gov/geo/). Differentially expressed genes (DEGs) were identified using the R package 'limma' (R version 4.3.0, limma version 3.58.1) under the threshold of absolute value of log2 fold change ≥1 and adjusted P<0.01. The protein expression of RNF125 in LUAD tissues was evaluated using the Human Protein Atlas database (https://www.proteinatlas.org/) (31). Pan-cancer analysis of RNF125 was performed using the TNMplot platform (https://tnmplot.com/) (32). RNF125 expression in different LUAD tumor stages was analyzed using the Tumor-Immune System Interactions Database web portal (http://cis.hku.hk/TISIDB/) (33). Survival analysis was performed using the GSE30219 (https://www.ncbi.nlm.nih.gov/geo/query/acc.cgi?acc=GSE30219) (34) and GSE11969 (https://www.ncbi.nlm.nih.gov/geo/query/acc.cgi?acc=GSE11969) (35,36) datasets via the PROGgeneV2 web portal (http://www.compbio.iupui.edu/proggene) (37).

The gene list of RNF125 interactors reported in at least two studies was downloaded from the BioGRID database (https://thebiogrid.org/) (38). A protein-protein interaction network of these RNF125 interactors was constructed using the GeneMANIA database (https://genemania.org/) (39). Gene Ontology Biological Process and Reactome pathway enrichment analysis of RNF125 interactors was performed using the DAVID database (https://davidbioinformatics.nih.gov/) (40). The gene list of RBPs with known pro- or anti-tumor functions in LC was downloaded from the GeneCards database (https://www.genecards.org/) (41). The potential RNF125-binding RBPs were predicted using two RBP databases: RBPDB (http://rbpdb.ccbr.utoronto.ca/) (26) and RBPmap (http://rbpmap.technion.ac.il/) (42). The gene list of human E3 ubiquitin ligases was downloaded from the UbiNet 2.0 database (https://awi.cuhk.edu.cn/~ubinet/index.php) (43). Correlation analysis between immune cell infiltration or RBP expression and RNF125 expression was performed using the TIMER2.0 database (http://timer.cistrome.org/) (25).

Cell culture. LUAD cell lines (NCI-H1975, NCI-H2228, NCI-H1395, HCC-827, CALU-3 and NCI-H1437), NK-92 and Jurkat T cells were purchased from iCell Bioscience, Inc. NCI-H1975 (cat. no. iCell-h156), NCI-H2228 (cat. no. iCell-h351), NCI-H1395 (cat. no. iCell-h154), HCC-827 (cat. no. iCell-h068), NCI-H1437 (cat. no. iCell-h284) and Jurkat T (cat. no. iCell-h117) cells were cultured in RPMI-1640 medium (Beijing Solarbio Science & Technology Co., Ltd.) containing 10% fetal bovine serum (FBS; Zhejiang Tianhang Biotechnology Co., Ltd.). CALU-3 cells were cultured in MEM medium (Procell Life Science & Technology Co., Ltd.) containing 10% FBS. NK-92 (cat. no. iCell-h0388) cells were maintained under dedicated culture conditions [MEMα (Wuhan Servicebio Technology Co., Ltd.) containing 12.5% FBS and 12.5% horse serum (Beijing Solarbio Science & Technology Co., Ltd.)]. Cells were cultured in a humidified 5% CO_2 atmosphere at 37˚C. All media were supplemented with 1% penicillin/streptomycin (cat. no. BL505A; Biosharp Life Sciences). All the cell lines were authenticated by short tandem repeats (STR) analysis.

Cell transfection. NCI-H1395 and HCC-827 cells were seeded into a 6-well plate 1 day prior to transfection. The cell transfection experiment was conducted when cells reached ~70% confluence. NCI-H1395 and HCC-827 cells were transfected with RNF125 overexpression plasmids or RNF125 small hairpin (sh)RNA or small interfering (si)RNAs targeting MBNL1 using Lipofectamine® 3000 reagent (Thermo Fisher Scientific, Inc.) according to the manufacturer's instructions. For each well, 2.5 μg of plasmids or 75 pmol of siRNA were added to cells for transfection. Cells were then incubated at 37˚C for 48 h, after which, cells were subjected to subsequent experiments. pcDNA3.1-EGFP vector and pGCsi-H1-Neo-GFP vector were obtained from Anhui General Biotech Co., Ltd. and were used for constructing RNF125 overexpression plasmid and RNF125 shRNA plasmid, respectively.

Stable cell lines were constructed by antibiotic selection and used for subsequent experiments. The shRNA and siRNA sequences used in the present study were as follows: shRNA negative control (shNC) sense, 5'-TTCTCCGAACGTGTCACGT-3' and antisense, 5'-ACGTGACACGTTCGGAGAA-3'; sh1-RNF125 sense, 5'-GAATGAAATCAGAGTATAA-3' and antisense, 5'-TTATACTCTGATTTCATTC-3'; sh2-RNF125 sense, 5'-GTCAGAAGTACATAGATAA-3' and antisense, 5'-TTATCTATGTACTTCTGAC-3'; si-NC sense, 5'-UUCUCC

GAACGUGUCACGU-3' and antisense, 5'-ACGUGACAC GUUCGGAGAA-3'; si1-MBNL1 sense, 5'-GCCAACCAG AUACCCAUAAUA-3' and antisense, 5'-UAUUAUGGGUAU CUGGUUGGC-3'; and si2-MBNL1 sense, 5'-GCCUGCUUU GAUUCAUUGAAA-3' and antisense, 5'-UUUCAAUGAAUC AAAGCAGGC-3'.

Reverse transcription-quantitative PCR (RT-qPCR). The extraction of RNA was performed using a standard phenol/chloroform protocol. NCI-H1395 and HCC-827 cells were lysed in 1 ml TRIpure Reagent (BioTeke Corporation). After incubation for 5 min at room temperature, 200 μl of chloroform was added, gently mixed and incubated for 3 min at room temperature. After centrifugation at 10,000 x g for 10 min at 4˚C, the aqueous phase was transferred to a new tube and an equal volume of isopropanol was added, mixed and incubated at -20˚C overnight. The samples were centrifuged at 10,000 x g for 10 min at 4˚C. The supernatant was discarded and 1 ml of 75% ethanol was added. After centrifugation at 3,400 x g for 3 min at 4˚C, the supernatant was discarded and the resulting RNA pellet was dried for 5 min at room temperature, then dissolved in 30 μl RNase-free ddH_2O. The concentration of RNA in each sample was determined using a UV-visible NanoDrop2000 spectrophotometer (Thermo Fisher Scientific, Inc.). The RNA samples were reverse transcribed into cDNA using random primers, RNase inhibitor (Biosharp Life Sciences), BeyoRT II M-MLV reverse transcriptase (Beyotime Institute of Biotechnology) and 5x reaction buffer provided with the reverse transcriptase. qPCR was performed using a qPCR instrument (Bioneer Corporation) using 1 μl cDNA template, 0.3 μl SYBR Green (Beijing Solarbio Science & Technology Co., Ltd.), 1 μl forward and reverse primers [General Biotech (Anhui) Co., Ltd.], 10 μl 2X Taq PCR Mastermix (Beijing Solarbio Science & Technology Co., Ltd) and ddH_2O. The amplification protocol was 95˚C for 5 min; 40 cycles of 95˚C for 10 sec, 60˚C for 10 sec and 72˚C for 15 sec; followed by the melt curve analysis for verification of primer specificity. The relative expression of target genes was normalized to β-actin. The data analyses were performed using the $2^{-\Delta\Delta Cq}$ method (44). The primer sequences were: β-actin forward (F), 5'-GCACAGAGCCTCGCCTT-3' and reverse (R), 5'-CCTTGCACATGCCGGAG-3'; MBNL1 F, 5'-AAAACG CAGTTGGAGATAA-3' and R, 5'-GAGAAACAGGTCCCA GATAG-3'; and RNF125 F, 5'-CTGCCGTTCCTGTATTG-3' and R, 5'-CACCTTGCTGCTGTCTC-3'.

Western blotting. After extracting the total protein from the cells using RIPA lysis buffer (Beijing Solarbio Science & Technology Co., Ltd) containing 1 mM PMSF (Beijing Solarbio Science & Technology Co., Ltd), a BCA protein assay kit (Beijing Solarbio Science & Technology Co., Ltd) was used to measure the protein concentrations. A total of 10-20 μg proteins were loaded per lane, separated by SDS-PAGE with 5% stacking gel and 8/13% separating gel and transferred to PVDF membranes (MilliporeSigma). The membranes were blocked with a Western blocking buffer (cat. no. SW3010; Beijing Solarbio Science & Technology Co., Ltd) at room temperature for 1 h, followed by incubation with primary antibodies against RNF125 (cat. no. DF4024; 1:1,000; Affinity Biosciences), cleaved poly ADP-ribose polymerase (PARP; cat. no. AF7023; 1:1,000; Affinity Biosciences), PD-L1 (cat. no. BF8035; 1:1,000; Affinity Biosciences), MBNL1 (cat. no. A8054; 1:1,000; ABclonal Biotech, Co., Ltd.) and β-actin (cat. no. 66009-1-Ig; 1:10,000; Proteintech Group, Inc.) at 4˚C overnight. The following day, the membranes were washed using TBST (0.15% Tween-20) and incubated with horseradish peroxidase-conjugated secondary antibodies goat anti-rabbit or anti-mouse IgG (cat nos. SE134 and SE131, respectively; 1:3,000; Beijing Solarbio Science & Technology Co., Ltd.) at 37˚C for 1 h. The blots were visualized using the ECL Western Blotting Substrate (Beijing Solarbio Science & Technology Co., Ltd) and analyzed with the Gel-Pro-Analyzer software (Media Cybernetics).

Colony formation assay. When the cultured NCI-H1395 and HCC-827 cells reached ~70% confluence, the cells were then subjected to trypsin digestion with 0.25% trypsin/0.02% EDTA for 2-5 min at 37˚C, centrifugation at 150 x g for 3 min at 4˚C and resuspension. The cells were seeded in the 6-cm cell culture dishes (300 cells/dish) and incubated for 2 weeks. Cells were fixed with 4% paraformaldehyde (Shanghai Aladdin Biochemical Technology Co., Ltd.) for 25 min at room temperature and then stained using a Wright-Giemsa composite stain kit for 5 min at room temperature (Nanjing Keygen Biotech, Co., Ltd.). After washing, an inverted phase-contrast microscope (Olympus Corporation) was used for cell photography and counting to calculate the colony formation efficiency: Colony formation efficiency (%)=(number of colonies/number of cells seeded) x100. Quantification was performed by manual counting under the microscope. Cell clusters containing >50 cells were counted as colonies.

Transwell invasion and migration assays. Transwell chambers (Beijing Landeco Technology Co., Ltd.) coated with (for invasion assay) or without (for migration assay) Matrigel (Corning, Inc.) at 37˚C for 2 h were placed into 24-well plates. A total of 800 μl culture medium containing 10% FBS was added to the lower chamber and 200 μl cell suspension (2,000 cells/well for migration assay and 20,000 cells/well for invasion assay) in serum-free RPMI-1640 medium was added to the upper chamber. After 24 h incubation at 37˚C, the cells that had migrated or invaded to the lower surface of the Transwell membrane were fixed with 4% paraformaldehyde for 20 min at room temperature, stained with crystal violet staining solution for 5 min at room temperature and imaged using an inverted light microscope (Olympus Corporation).

Cisplatin sensitivity assay. NCI-H1395 and HCC-827 cells were treated with different concentrations of cisplatin (0.0, 0.5, 1.0, 2.0, 5.0, 10.0, 20.0 and 50.0 μM; Dalian Meilun Biology Technology Co., Ltd.) for 48 h at 37˚C. Cisplatin-induced changes in cell viability were measured with the MTT assay.

MTT assay. NCI-H1395 and HCC-827 Cells were inoculated in 96-well plates at $5x10^3$ cells/well and cultured for 0, 24, 48 and 72 h. Each group was set up with 5 multiple wells. At the indicated time points, 50 μl MTT staining solution was added to each well (Nanjing Keygen Biotech, Co., Ltd.) and incubated for 4 h at 37˚C. The supernatant was aspirated and 150 μl DMSO (Nanjing Keygen Biotech, Co., Ltd.) was added

to dissolve the purple-colored formazan crystals. The optical density was measured at 490 nm using an Enzyme-labeled Instrument (BioTek; Agilent Technologies, Inc.).

Caspase-3 activity assay. Caspase-3 activity was measured using the Caspase-3 Activity Assay Kit (cat. no. C1116; Beyotime Institute of Biotechnology) according to the manufacturer's protocol. The measurement of caspase-3 activity is based on the ability of caspase-3 to change Ac-DEVD-*p*NA into the yellow formazan product, *p*-nitroaniline (*p*NA). NCI-H1395 and HCC-827 cells were lysed with lysis buffer included in the kit in an ice bath for 15 min and centrifuged at 16,000 x g for 15 min at 4˚C. The supernatant was incubated with Ac-DEVD-*p*NA (caspase-3 substrate) at 37˚C for 2 h. Caspase-3 activity was measured by spectrophotometric detection of *p*NA at a wavelength of 405 nm.

Co-immunoprecipitation (Co-IP). The total protein extraction was performed as described in the western blotting section. The total protein concentration was determined using the BCA Protein Assay Kit (Beyotime Institute of Biotechnology) following the manufacturer's instructions. Co-IP analysis was performed according to the manufacturer's instructions for Pierce Co-IP Kit (cat. no. 26149, Thermo Fisher Scientific, Inc.). For each IP reaction, 2 μg anti-PD-L1 antibodies (cat. no. BF8035; 1:100; Affinity Biosciences) or negative control IgG (cat. no. A7016; 1:100; Beyotime) were crosslinked to 20 μl AminoLink Plus Coupling Resin slurry. A total of 500 μg lysates were incubated with the antibody-coupled resin at 4˚C overnight. The following day, the samples were washed using 200 μl IP Lysis/Wash buffer, 200 μl Modified Dulbecco's PBS and 100 μl Conditioning Buffer included in the Co-IP kit and the flow-through was discarded. Next, the immunoprecipitates were washed with 10 μl Elution Buffer included in the Co-IP kit. Subsequently, 50 μl Elution Buffer was added and incubated for 5 min at room temperature. Finally, the tube was briefly centrifuged, and the flow-through was collected. The protein samples were separated by SDS-PAGE as described in the western blotting section.

Evaluation of Jurkat T cell activation. Evaluation of Jurkat T cell activation was performed as previously described (18). Jurkat T cells were resuspended in basal culture medium (RPMI-1640 + 10% FBS) containing 20 ng/ml phorbol 12-myristate 13-acetate and 200 μg/ml ionomycin and co-cultured with LUAD (NCI-H1395 and HCC-827) cells. The ratio of cancer cells to T cells was 1:4. The level of IL-2 in the cell culture supernatants was determined using an ELISA kit (cat. no. EK102; Hangzhou Lianke Biotechnology Co., Ltd.) according to the manufacturer's protocol.

NK cell cytotoxicity assay. NK cell cytotoxicity assay was performed as previously described (17). In brief, NK-92 cells were co-cultured with LUAD (NCI-H1395 and HCC-827) cells at different cancer cell to NK cell ratios (1:0, 1:2.5, 1:5 and 1:10) for 4 h. The viability of cancer cells was detected by MTT assay after refreshing the culture medium to remove NK cells.

RNA stability analysis. RNA stability analysis was performed as previously described (45). Cells were transfected with MBNL1 siRNA or the corresponding control siRNA. A total of 48 h after cell transfection, the cells were treated with 5 mg/ml actinomycin D for different times at 37˚C (0, 1, 2.5 and 5 h). qPCR was performed to detect RNF125 mRNA levels, using 18S rRNA as the endogenous normalization control as previously described (46). The primer sequences of 18S rRNA were: F, 5'-AGCGAAAGCATTTGCCAAGA-3' and R, 5'-TATGGT CGGAACTACGACGGT-3'. The percentage of remaining RNF125 mRNA relative to 0 h at the indicated time points was calculated.

RNA immunoprecipitation (RIP)-PCR. RIP-PCR experiments were performed to verify the binding of the MBNL1 protein to the RNF125 transcript. The cells were resuspended in RIP lysis buffer (MilliporeSigma). A total of 5 μg anti-MBNL1 antibodies (cat. no. A8054, 1:1,000; ABclonal Biotech Co., Ltd.) were pre-bound to Protein A/G magnetic beads in immunoprecipitation buffer and then incubated with cell lysates for 12 h at 4˚C. After washing the magnetic beads, the RNA-protein complex was added to the proteinase K buffer included in the RIP kit (cat. no. 17-701; MilliporeSigma). The extraction of RNA was performed using a standard phenol/chloroform protocol as previously described in the RT-qPCR section of the manuscript. The extracted RNA was reverse transcribed to cDNA using BeyoRT II M-MLV reverse transcriptase (Beyotime Institute of Biotechnology) according to the manufacturer's instructions. The resulting cDNA was used as the template for PCR. The primer sequences were: F, 5'-AAAAGGGACCACTGAAT-3' and R, 5'-CACCTACTT GCCTACCA-3'. The amplification protocol was 95˚C for 5 min; 40 cycles of 95˚C for 15 sec, 55˚C for 25 sec and 72˚C for 30 sec; followed by 25˚C for 5 min. The PCR product was electrophoresed on a 2% agarose gel. Electrophoresis images were obtained using a gel imaging analysis system (Beijing LIUYI Biotechnology Co., Ltd.

Immunohistochemical (IHC) staining and analysis. A total of 21 pairs of non-cancerous and cancerous tissues were collected from patients with LUAD [8 men and 13 women; median age, 64 years (range, 32-74 years)] who underwent surgery at the Harbin Medical University Cancer Hospital (Harbin, China) in December 2024. These samples were collected as part of an overall project on IHC staining and analysis of lung cancer specimens.

Tissue specimens were fixed with 4% paraformaldehyde for 24 h at 4˚C, embedded with paraffin and sliced at a 5-μm thickness. The sections were then deparaffinized by baking at 64˚C for 2-4 h and xylene and rehydrated by transfer through a decreasing concentration gradient of ethanol solutions. After antigen retrieval, the sections were incubated with 3% H_2O_2 solution for 15 min at room temperature to block the endogenous peroxidase activity. Prior to immunostaining with primary antibodies against RNF125 (cat. no. 13290-1-AP; 1:50; Proteintech Group, Inc.), the sections were blocked with 1% bovine serum albumin for 15 min at room temperature (Sangon Biotech Co., Ltd.). After overnight incubation with the primary antibodies at 4˚C, the sections were washed and incubated with the HRP-conjugated secondary goat anti-rabbit IgG antibodies (cat. no. 31460; 1:500; Thermo Fisher Scientific, Inc.) at 37˚C for 1 h. The IHC signal was

developed by 3,3'-diaminobenzidine substrates. The sections were incubated in hematoxylin for 3 min at room temperature for counterstaining. After which, the sections were observed under a light microscope. The signal intensity and percentage of stained cells were measured as previously described (47). The staining intensity was manually scored from 0 (lowest) to 3 (highest). The number of stained cells was counted using the Image-Pro Plus version 6.0 software (Media Cybernetics). The IHC score was determined by the percentage of stained cells multiplied by the staining intensity (IHC score=percentage of stained cells x staining intensity).

Statistical analysis. Data were presented as the mean ± standard deviation (SD) and analyzed using the GraphPad Prism (version 9; Dotmatics). Each experiment was repeated in triplicate. The Wilcoxon matched pairs signed rank test was used to compare the differences between the IHC staining scores of RNF125. Unpaired student's t-tests were used to examine the differences between two groups. A one- or two-way ANOVA with Tukey's multiple comparison test was used to compare the means of ≥3 groups. $P<0.05$ was considered to indicate a statistically significant difference.

Results

RNF125 is downregulated in human LC and predicts unfavorable survival. To identify the differentially expressed E3 ubiquitin ligases in LUAD, first three GSE cohorts GSE75037 (27), GSE31210 (28,29) and GSE116959 (30) containing LUAD and corresponding non-cancer samples were analyzed. After which, the differentially expressed genes (DEGs; absolute value of log2 fold change ≥1 and adjusted $P<0.01$) were overlapped with the gene list of human E3 ubiquitin ligases downloaded from the UbiNet 2.0 database (https://awi.cuhk.edu.cn/~ubinet/index.php) (43). As a result, 10 E3 ubiquitin ligases were found to be differentially expressed in LUAD (Fig. 1A). The functions of most of these ligases have been previously reported in LC (48-56), with only RNF125 identified as a novel DEG in LC (Fig. 1A). The expression of RNF125 was downregulated in LUAD samples compared with non-cancerous samples (Fig. 1B). Subsequently, IHC staining was performed for RNF125 in 21 pairs of LUAD tissue and adjacent non-cancerous tissue. Compared with the non-cancerous tissues, LUAD tissues had a lower IHC score for RNF125, suggesting that RNF125 was downregulated in human LUAD tissues (Fig. 1C). Similarly, the Human Protein Atlas database (https://www.proteinatlas.org/) (31) was explored to assess the protein expression of RNF125 in LUAD tissues, showing a low staining of RNF125 in LUAD, which was consistent with the present results (Fig. 1D).

Next, a pan-cancer analysis of RNF125 was performed using the TNMplot platform and it was demonstrated that RNF125 was significantly downregulated in several cancers including LC (Fig. 2A) (32). Moreover, RNF125 expression was significantly gradually decreased in normal lung tissues, primary tumor and metastatic LC tissues (Fig. 2B) (32). After which, RNF125 expression was analyzed in different LUAD tumor stages via the TISIDB web portal (http://cis.hku.hk/TISIDB/) (33). These results showed a weak negative association between RNF125 expression and LUAD tumor stage (Fig. 2C). Survival analysis was performed using two GSE cohorts: GSE30219 (https://www.ncbi.nlm.nih.gov/geo/query/acc.cgi?acc=GSE30219) (34) and GSE11969 (https://www.ncbi.nlm.nih.gov/geo/query/acc.cgi?acc=GSE11969) (35,36) via the PROGgeneV2 web portal (http://www.compbio.iupui.edu/proggene) (37). The results indicated that increased expression of RNF125 was associated with high overall survival of patients (Fig. 2D). These data suggested that RNF125 expression was decreased in LC and that reduced RNF125 levels predicted unfavorable survival.

RNF125 inhibits proliferation, colony formation, migration and invasion of LUAD cells. The expression of RNF125 in LUAD cells was detected by RT-qPCR. NCI-H1975 and NCI-H2228 cells showed the highest levels of RNF125 expression; CALU-3 and NCI-H1437 cells showed the lowest levels of RNF125 expression; and NCI-H1395 and HCC-827 cells showed moderate RNF125 expression levels (Fig. 3A). Since the present study intended to determine the effects of RNF125 deficiency or overexpression on the same LUAD cell line, NCI-H1395 and HCC-827 cells with moderate RNF125 expression were selected to establish RNF125-silenced and RNF125-overexpressing cell lines for subsequent experiments. To address the role of RNF125 in LUAD, RNF125 overexpression or stable knockdown LUAD cells were constructed to evaluate the effect of RNF125 on the proliferation, colony formation, migration and invasion of LUAD cells. The results of RT-qPCR and western blotting demonstrated that RNF125 was effectively overexpressed or knocked down (Fig. 3B and C). Compared with the sh-NC group, silencing of RNF125 significantly promoted proliferation of LUAD cells (Fig. 3D). Conversely, compared with the Vector group, the overexpression of RNF125 significantly inhibited proliferation of LUAD cells (Fig. 3E). Compared with the sh-NC group, RNF125 silencing significantly promoted colony formation of NCI-H1395 cells and compared with the Vector group, RNF125 overexpression significantly inhibited colony formation of NCI-H1395 cells (Fig. 3F) Similar results were observed in HCC-827 cells (Fig. 3G).

As demonstrated by the Transwell migration assay results, the cell migration capacity was significantly enhanced in RNF125-silenced NCI-H1395 cells compared with the sh-NC group and suppressed in RNF125-overexpressing NCI-H1395 cells compared with the Vector group (Fig. 4A). Similar results were observed in HCC-827 cells as well (Fig. 4B). Additionally, the capabilities of cell invasion were significantly enhanced in RNF125-silenced LUAD cells compared to the sh-NC group and suppressed in RNF125-overexpressing LUAD cells compared to the Vector group (Fig. 4C and D).

Taken together, these data suggested that RNF125 suppressed proliferation, colony formation, migration and invasion of LUAD cells.

RNF125 enhances the efficacy of cisplatin in LUAD cells. The role of RNF125 in the sensitization of LUAD cells to cisplatin was investigated. Cells were treated with different concentrations of cisplatin for 48 h and the MTT assay was used to detect cell viability to calculate the relative inhibition rate. After treatment with each indicated concentration of cisplatin,

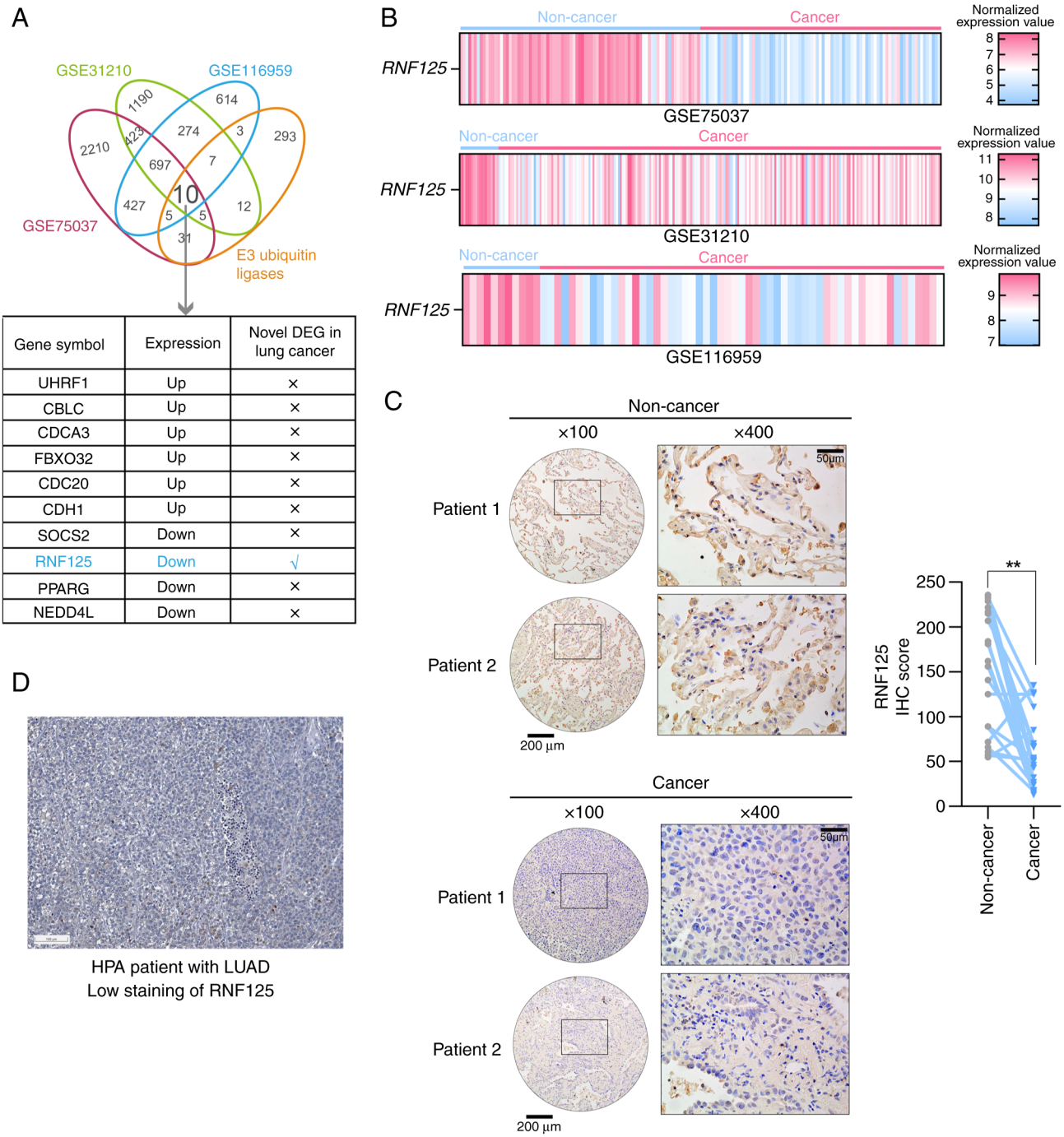

Gene symbol	Expression	Novel DEG in lung cancer
UHRF1	Up	×
CBLC	Up	×
CDCA3	Up	×
FBXO32	Up	×
CDC20	Up	×
CDH1	Up	×
SOCS2	Down	×
RNF125	Down	√
PPARG	Down	×
NEDD4L	Down	×

Figure 1. E3 ubiquitin ligase RNF125 is downregulated in LC. (A) GSE datasets showing the expression profile of LUAD and non-cancer samples were downloaded and analyzed. DEGs in these three datasets were overlapped with the gene list of human E3 ubiquitin ligases downloaded from the UbiNet 2.0 database. A total of 10 overlapping genes were identified and RNF125 was the only novel gene in LC. (B) The heatmap shows the expression of RNF125 in the three datasets. (C) Representative images of IHC staining for RNF125 in 21 pairs of LUAD tissues and adjacent non-cancerous tissues are shown. Scale bar, 200 or 50 μm. The statistical analysis result of the IHC score is shown in the right panel. **P<0.01. (D) The representative image of immunohistochemical staining of RNF125 in LUAD tissues was downloaded from HPA. RNF125, ring finger protein 125; LUAD, lung adenocarcinoma; LC, lung cancer; DEG, differentially expressed gene; HPA, Human Protein Atlas.

the inhibitory effect of cisplatin on LUAD cell viability was significantly decreased in RNF125-silenced cells and significantly promoted in RNF125-overexpressing cells compared with the corresponding control groups (sh-NC group or Vector group) (Fig. 5A and B). Furthermore, compared with the corresponding control groups (sh-NC group or Vector group), the caspase-3 levels in cisplatin-treated LUAD cells were significantly reduced by RNF125 knockdown (Fig. 5C) but increased by RNF125 overexpression (Fig. 5D). Similarly, compared with the corresponding control groups (sh-NC group or Vector group), the protein expression levels of cleaved PARP in cisplatin-treated LUAD cells was significantly reduced by RNF125 knockdown (Fig. 5E) but increased by RNF125 overexpression (Fig. 5F). Collectively, these results showed that RNF125 enhanced the sensitivity of LUAD cells to cisplatin.

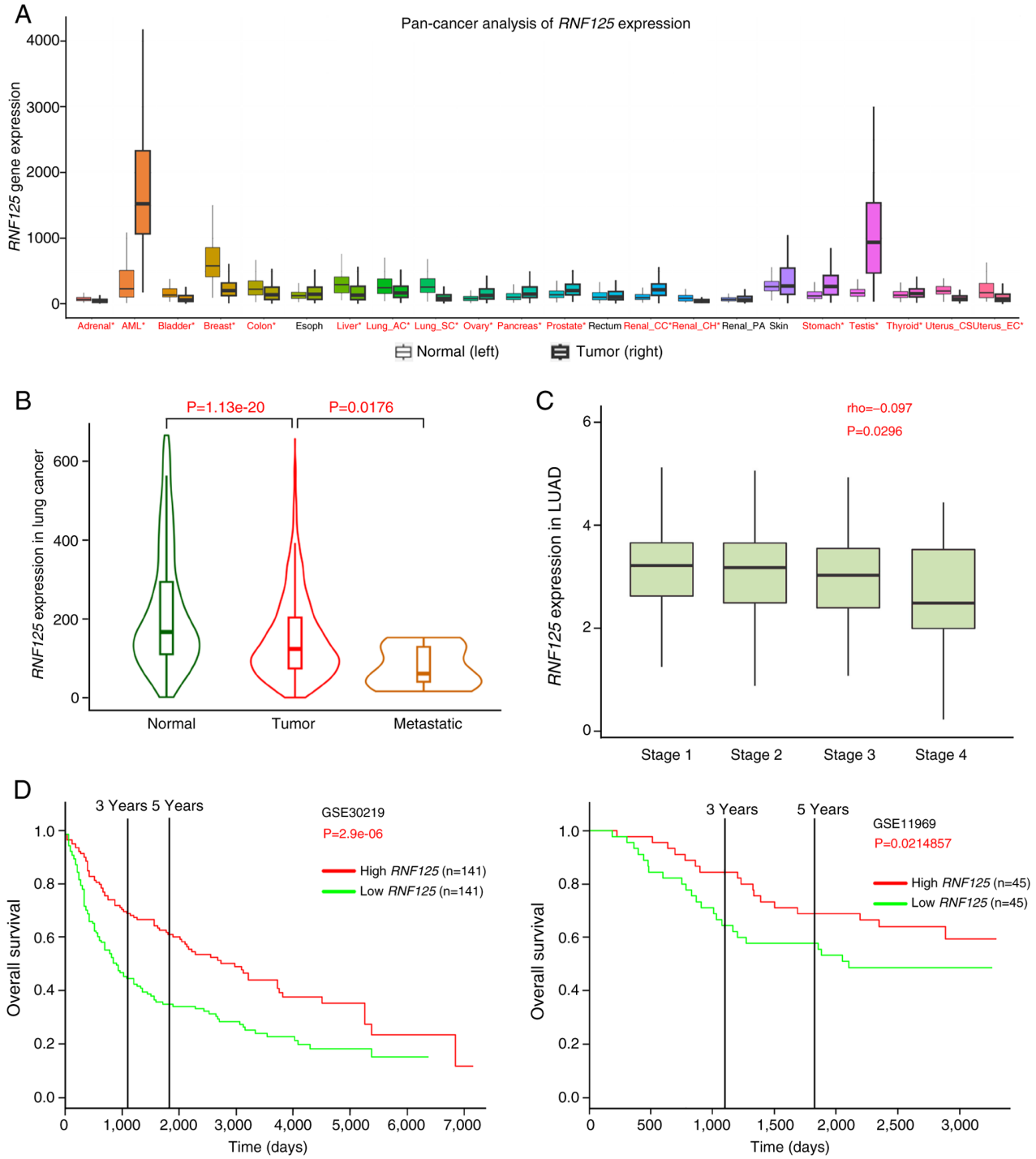

Figure 2. Clinical significance of RNF125 expression in human LC. (A) Pan-cancer analysis of RNF125 expression was performed using the TNMplot platform. (B) RNF125 expression analysis based on the metastatic status of LC was performed using the TNMplot platform. (C) The association between RNF125 expression and LUAD tumor stage was performed using the TISIDB web portal. Spearman correlation analysis was performed using data from all tumor stages. (D) Overall survival analysis based on RNF125 expression levels was performed using the Gene Expression Omnibus datasets via the PROGgeneV2 database. RNF125, ring finger protein 125; LUAD, lung adenocarcinoma; LC, lung cancer.

RNF125 knockdown in LUAD cells increases PD-L1, suppresses T-cell activation and attenuates NK cell killing of cancer cells. To investigate the downstream molecular mechanism of RNF125 in LUAD, the RNF125 interactors reported by at least two studies were downloaded from the BioGRID database (https://thebiogrid.org/) (38). A protein-protein interaction network of these RNF125 interactors was constructed using the GeneMANIA database (https://genemania.org/) (39), in which CD274 (also termed PD-L1) was identified as an important interactor of RNF125 (Fig. 6A). Gene Ontology Biological Process and Reactome pathway enrichment analysis revealed that these RNF125 interactors were markedly enriched in protein ubiquitination and immune response-related processes and pathways (Fig. 6B). These findings were consistent with a previous study showing that RNF125 facilitated PD-L1 ubiquitination and degradation

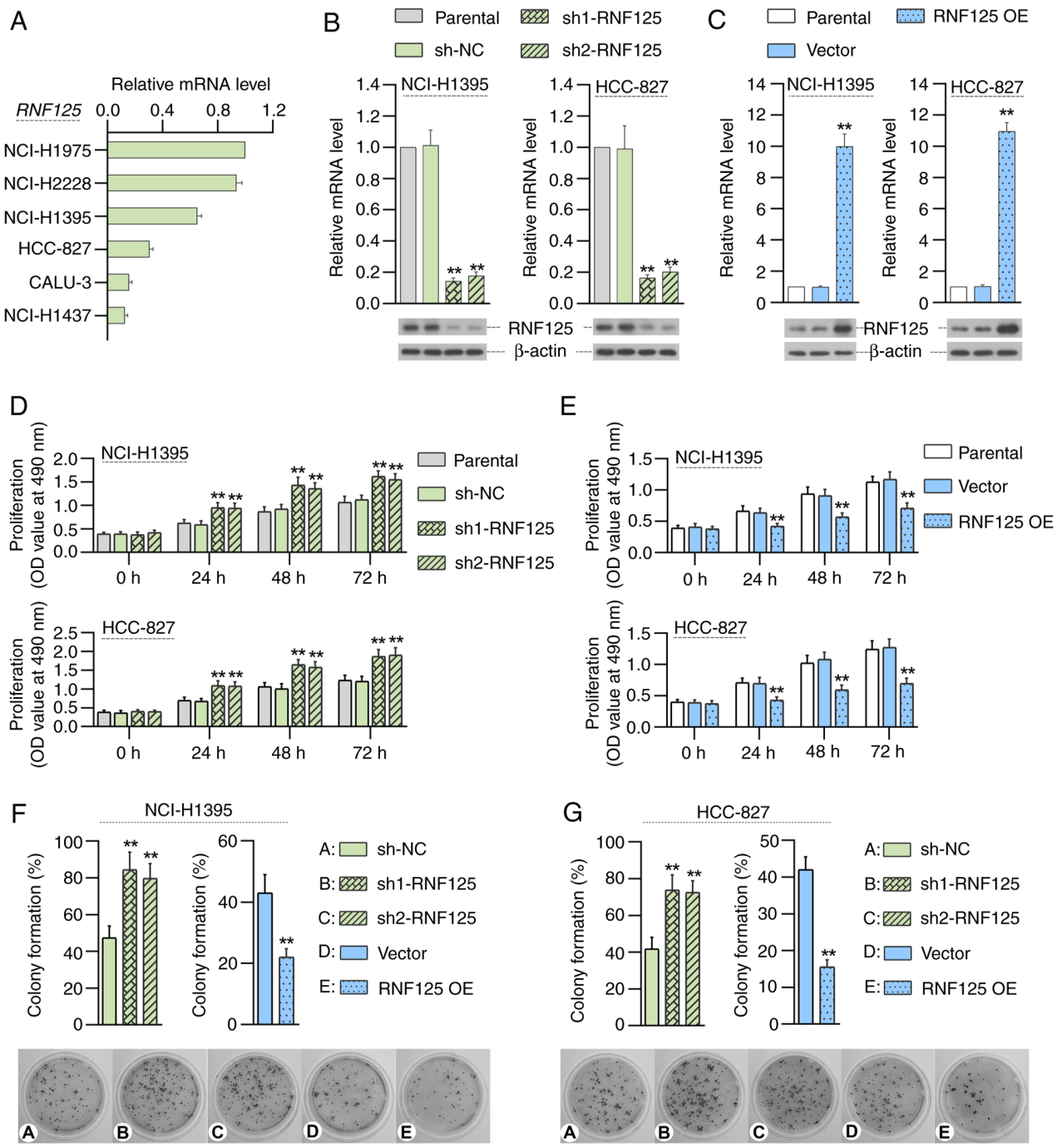

Figure 3. RNF125 inhibits the proliferation and colony formation of LUAD cells. (A) RT-qPCR shows RNF125 expression in six LC cell lines (NCI-H1975, NCI-H2228, NCI-H1395, HCC-827, CALU-3 and NCI-H1437). RT-qPCR and western blotting demonstrate plasmid-mediated RNF125 (B) knockdown or (C) overexpression in NCI-H1395 and HCC-827 cells. MTT assays show the effect of RNF125 (D) knockdown or (E) overexpression on the proliferation of NCI-H1395 and HCC-827 cells. Colony formation analysis shows the effect of RNF125 knockdown or overexpression on colony formation of (F) NCI-H1395 and (G) HCC-827 cells. Data are presented as mean ± SD. **P<0.01 vs. shNC or vector. LUAD, lung adenocarcinoma; RT-qPCR, reverse transcription-quantitative PCR; RNF125, ring finger protein 125; sh, short hairpin RNA; NC, negative control; OE, overexpression; OD, optical density.

and thereby suppressed immune evasion in head and neck squamous cell carcinoma (14).

To investigate the effect of RNF125 on PD-L1 expression, Co-IP and western blotting assays were performed. Co-IP assay results confirmed the interaction between RNF125 and PD-L1 (Fig. 6C). The results of the western blotting indicated that RNF125 silencing increased the expression of PD-L1 (Fig. 6D).

The TIMER2.0 database (http://timer.cistrome.org/) (25) was used to investigate the association between RNF125 expression and immune cell infiltration in LUAD. A positive correlation was observed between RNF125 expression and $CD8^+$ T cell, NK cell and M1/M2 macrophage infiltration levels in LUAD, suggesting the potential involvement of RNF125 in tumor immunity in LUAD (Fig. 6E).

Additionally, the effect of RNF125 knockdown on the anti-tumor activity of Jurkat T cells and NK-92 cells was evaluated. Compared with those co-cultured with sh-NC LUAD cells, the activated Jurkat T cells co-cultured with RNF125-silenced

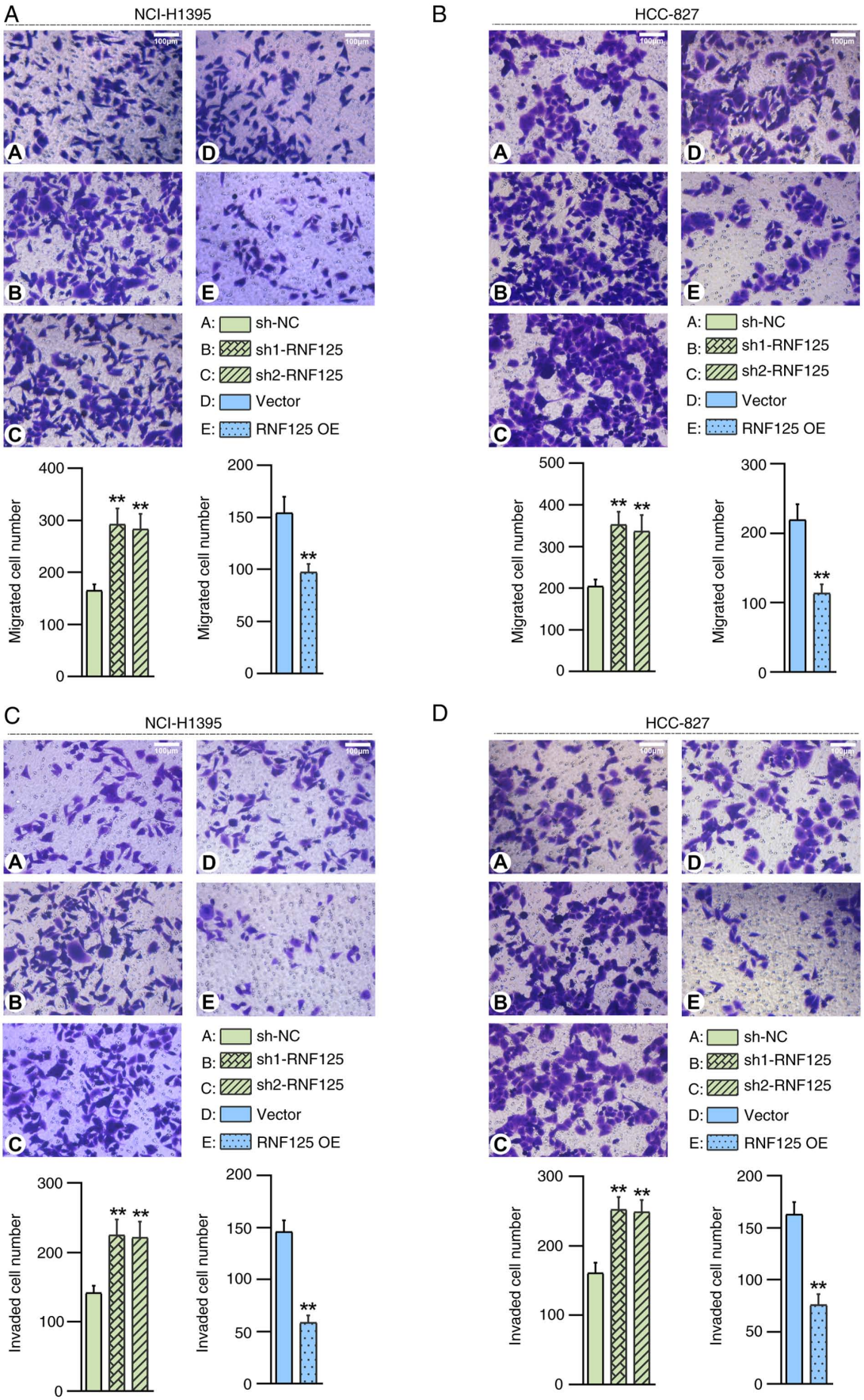

Figure 4. RNF125 inhibits migration and invasion of NCI-H1395 and HCC-827 cells. Transwell assays in the absence of Matrigel show the effect of RNF125 on the migration of (A) NCI-H1395 and (B) HCC-827 cells. Representative images (top) and the mean number of migrated cells (bottom) are shown. Transwell assays in the presence of Matrigel show the effect of RNF125 on the invasion of (C) NCI-H1395 and (D) HCC-827 cells. Representative images (top) and the mean number of invaded cells (bottom) are shown. Scale bar, 100 μm. Data are presented as mean ± SD. **P<0.01 vs. shNC or vector. RNF125, ring finger protein 125; sh, short hairpin RNA; NC, negative control; OE, overexpression.

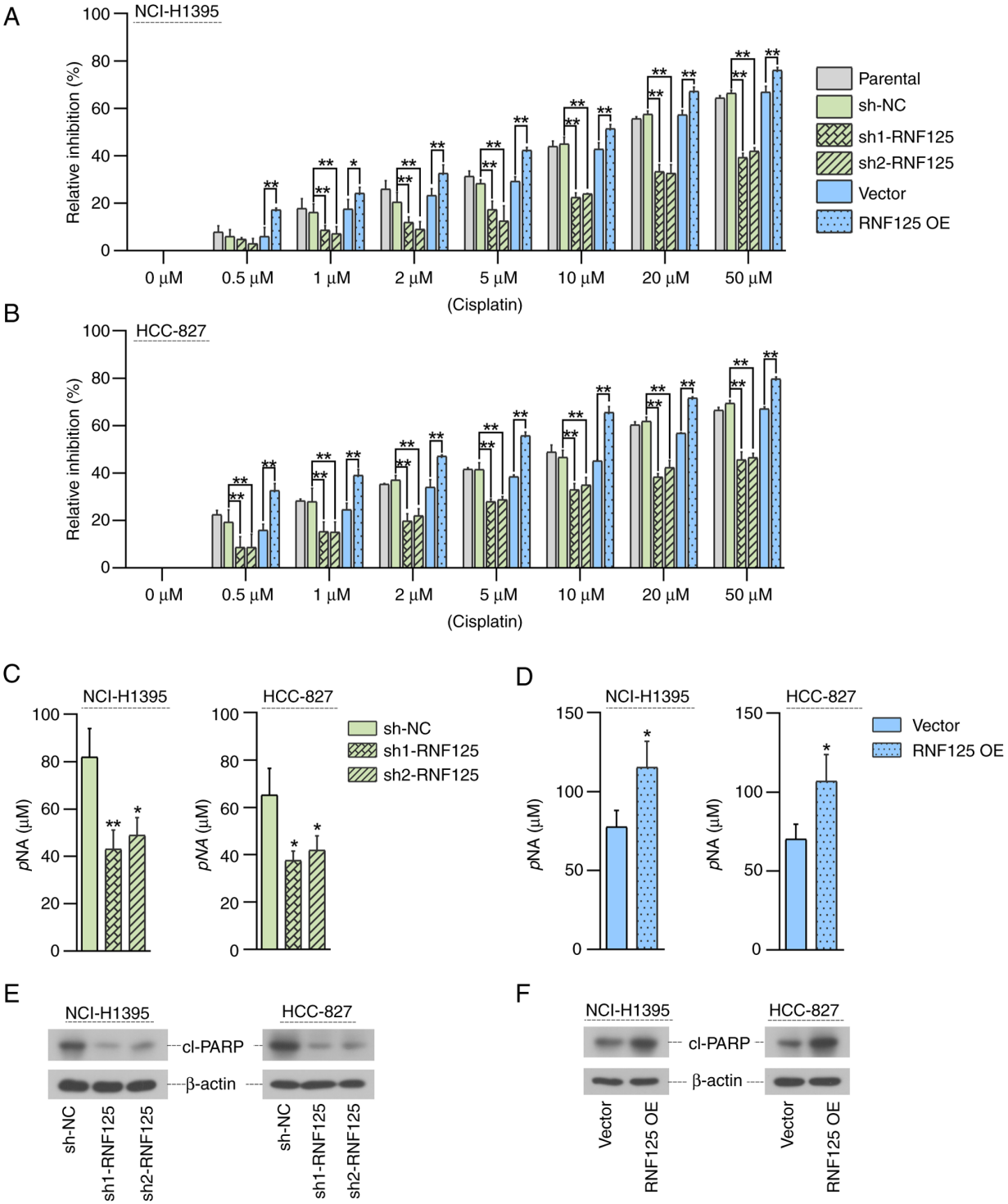

Figure 5. RNF125 increases the sensitivity of NCI-H1395 and HCC-827 cells to cisplatin. MTT assays show the effect of RNF125 on the sensitivity of (A) NCI-H1395 and (B) HCC-827 cells to cisplatin at the indicated time points. Quantitative analysis demonstrates the effect of RNF125 (C) knockdown or (D) overexpression on caspase-3 activity in NCI-H1395 and HCC-827 cells in the presence of cisplatin. The concentration of *p*NA indicates the activity of caspase-3. Western blotting determines the levels of cleaved PARP in (E) RNF125-silenced or (F) RNF125-overexpressing NCI-H1395 and HCC-827 cells in the presence of cisplatin. Data are presented as mean ± SD. *P<0.05, **P<0.01 vs. shNC or vector. RNF125, ring finger protein 125; PARP, poly(ADP-ribose) polymerase; *p*NA, *p*-nitroaniline; sh, short hairpin RNA; NC, negative control; OE, overexpression.

LUAD cells released significantly lower IL-2 (Fig. 6F). Similarly, co-culture with NK cells resulted in the death of sh-NC LUAD cells, which was significantly suppressed in the LUAD cells with RNF125 knockdown (Fig. 6G). Taken together, the loss of RNF125 enhanced the immune escape of LUAD cells.

MBNL1 is an upstream regulator of RNF125 in LUAD. To investigate the molecular mechanism underlying RNF125 expression regulation in LUAD, the potential RNF125-binding RBPs were predicted using two RBP databases RBPDB (http://rbpdb.ccbr.utoronto.ca/) (26) and RBPmap (http://rbpmap.technion.ac.il/) (42). In addition, the RBPs with

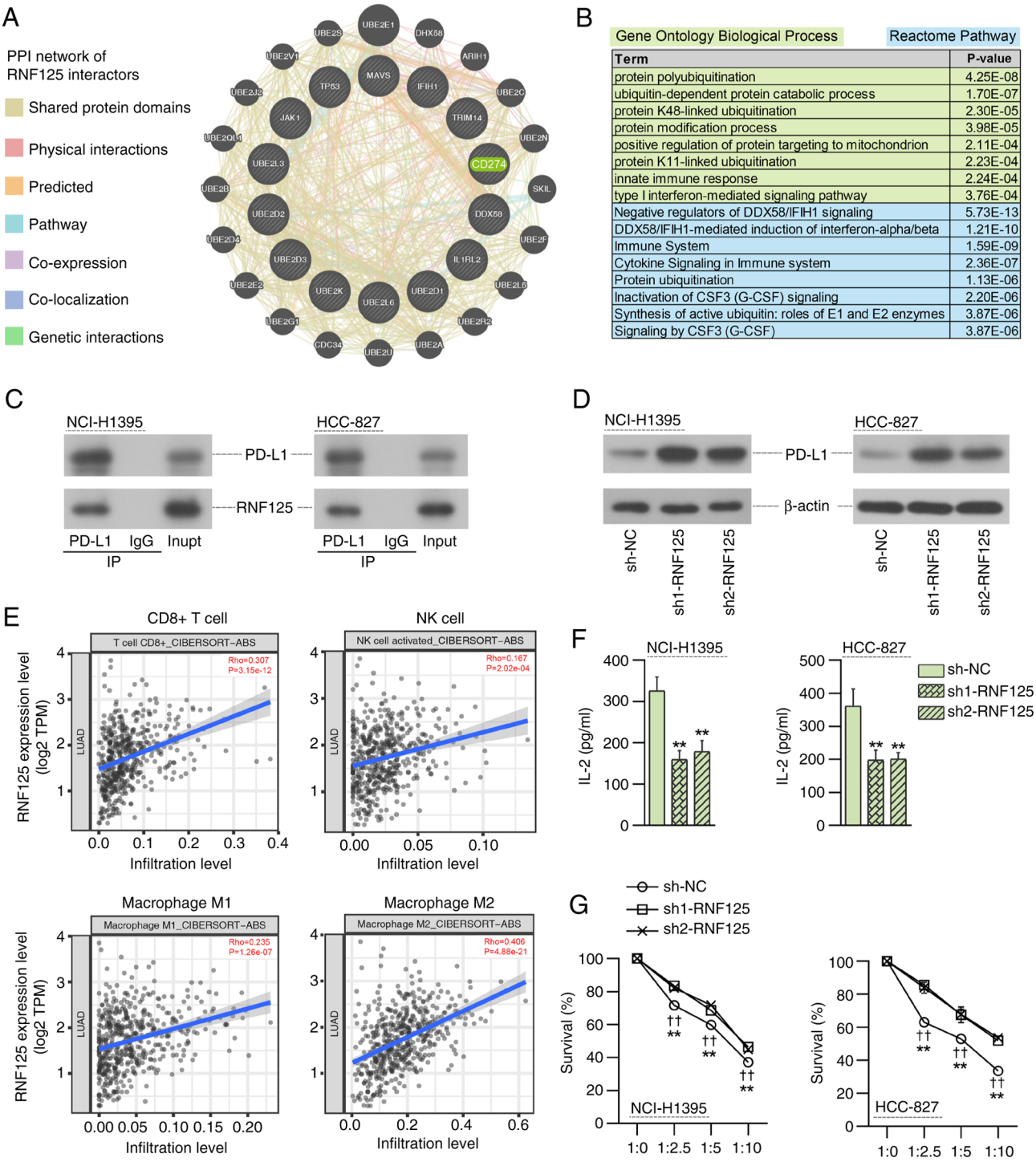

Figure 6. Knockdown of RNF125 enhances immune evasion in LUAD. (A) The PPI network of RNF125 interactors was constructed using the GeneMANIA database. (B) Gene Ontology Biological Process and Reactome pathway enrichment analysis of RNF125 interactors was performed using the DAVID database. (C) Co-IP assays show the interactions between RNF125 and PD-L1 in NCI-H1395 and HCC-827 cells. (D) Western blotting determines that knockdown of RNF125 reduces PD-L1 protein expression levels in NCI-H1395 and HCC-827 cells. (E) Correlation analysis between RNF125 expression and immune cell infiltration in LUAD was performed using the TIMER2.0 database. (F) Co-culture of T cells and RNF125-silenced cancer cells decreased IL-2 secretion from T cells. **P<0.01 vs. shNC. (G) Co-culture of NK cells and RNF125-silenced cancer cells attenuated NK cell-mediated lysis of NCI-H1395 and HCC-827 cells. **P<0.01 vs. sh1-RNF125; ††P<0.01 vs. sh2-RNF125. Data are presented as mean ± SD. PPI, protein-protein interaction; RNF125, ring finger protein 125; PD-L1, programmed cell death 1 ligand 1; LUAD, lung adenocarcinoma; sh, short hairpin RNA; NC, negative control; NK, natural killer; TPM, transcripts per million.

known pro-tumor or anti-tumor functions in LC were searched for in the GeneCards database (https://www.genecards.org/) (41). A total of five RNF125-binding RBPs were obtained (Fig. 7A). Furthermore, expression correlation analysis was performed between RNF125 and these RBPs in LUAD using the TIMER2.0 database and it was found that MBNL1 had the highest correlation coefficient with RNF125 in LUAD (Fig. 7B). Therefore, MBNL1 was selected for further study.

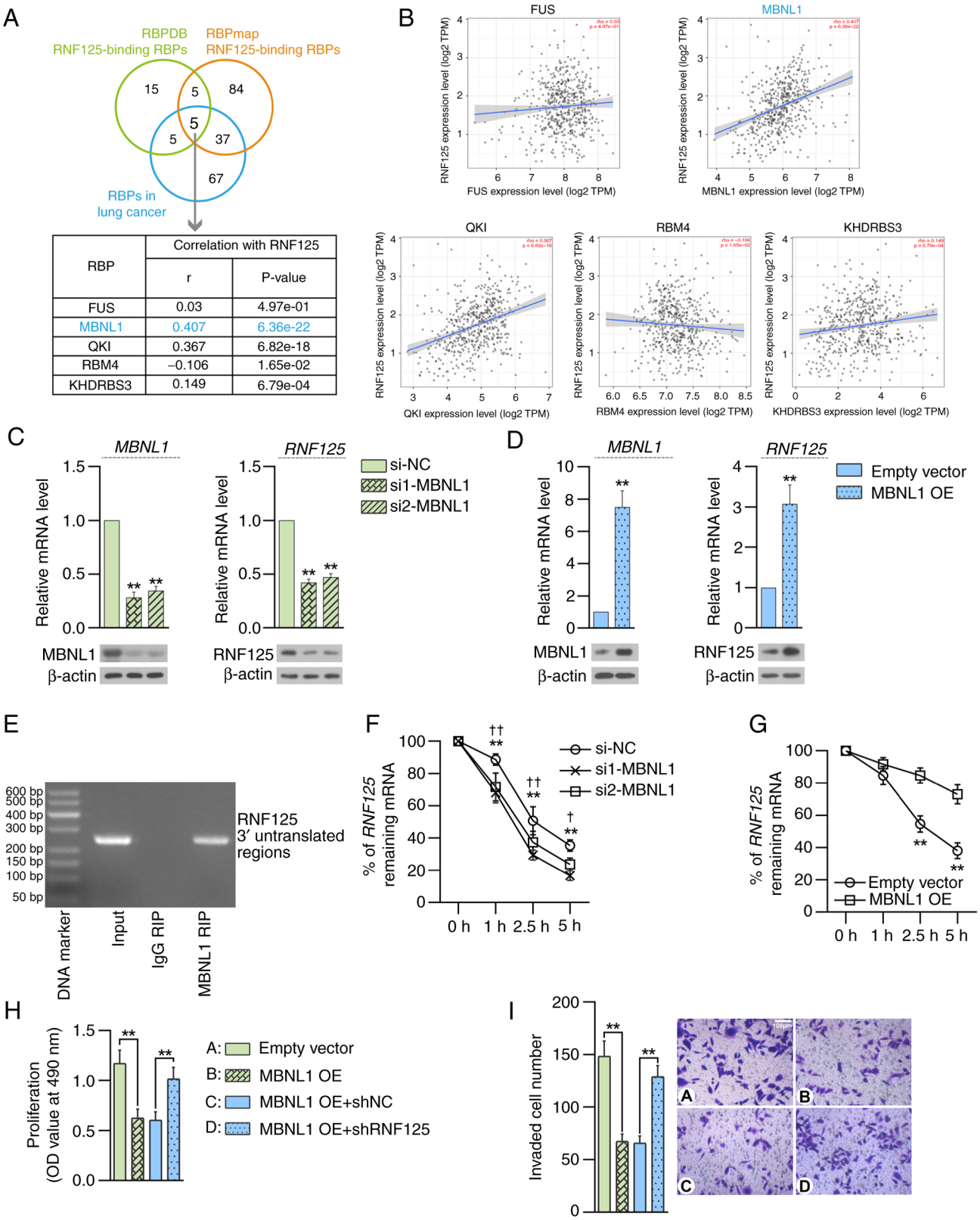

RBP	Correlation with RNF125	
	r	P-value
FUS	0.03	4.97e-01
MBNL1	0.407	6.36e-22
QKI	0.367	6.82e-18
RBM4	−0.106	1.65e-02
KHDRBS3	0.149	6.79e-04

Figure 7. MBNL1 is an upstream modulator of RNF125 in LUAD. (A) Potential RNF125-binding RBPs were predicted using two RBP databases (RBPDB and RBPmap) and overlapped with RBPs involved in lung cancer progression. (B) Correlation analysis between RNF125 and the indicated RBPs in LUAD was performed using the TIMER2.0 portal. RT-qPCR and western blotting show MBNL1 and RNF125 expression in NCI-H1395 cells 48 h after transfection of (C) MBNL1-specific siRNAs or (D) plasmids containing MBNL1 coding sequences (MBNL1 OE). **P<0.01 vs. siNC or empty vector. (E) RIP-PCR and agarose gel electrophoresis showed that RNF125 transcripts were detected in the MBNL1 antibody RIP products from NCI-H1395 cells. After treatment with actinomycin D, RT-qPCR analysis showed the % of remaining RNF125 mRNA relative to 0 h at the indicated time points in (F) MBNL1-silenced (**P<0.01 vs. si1-MBNL1; †P<0.05, ††P<0.01 vs. si2-MBNL1) or (G) MBNL1-overexpressing NCI-H1395 cells (**P<0.01 vs. empty vector). (H) MTT assays determine the viability of NCI-H1395 cells 48 h after co-transfection of MBNL1 OE and shRNF125 plasmids. (I) Representative images (right) of Transwell assays in the presence of Matrigel and the mean number of invaded cells (left) are shown. Scale bar, 100 μm. **P<0.01. Data are presented as mean ± SD. MBNL1, muscleblind-like 1; RNF125, ring finger protein 125; LUAD, lung adenocarcinoma; RBP, receptor binding protein; RT-qPCR, reverse transcription-quantitative PCR; siRNA, small interfering RNA; OE, overexpression; NC, negative control; sh, short hairpin RNA; TPM, transcripts per million.

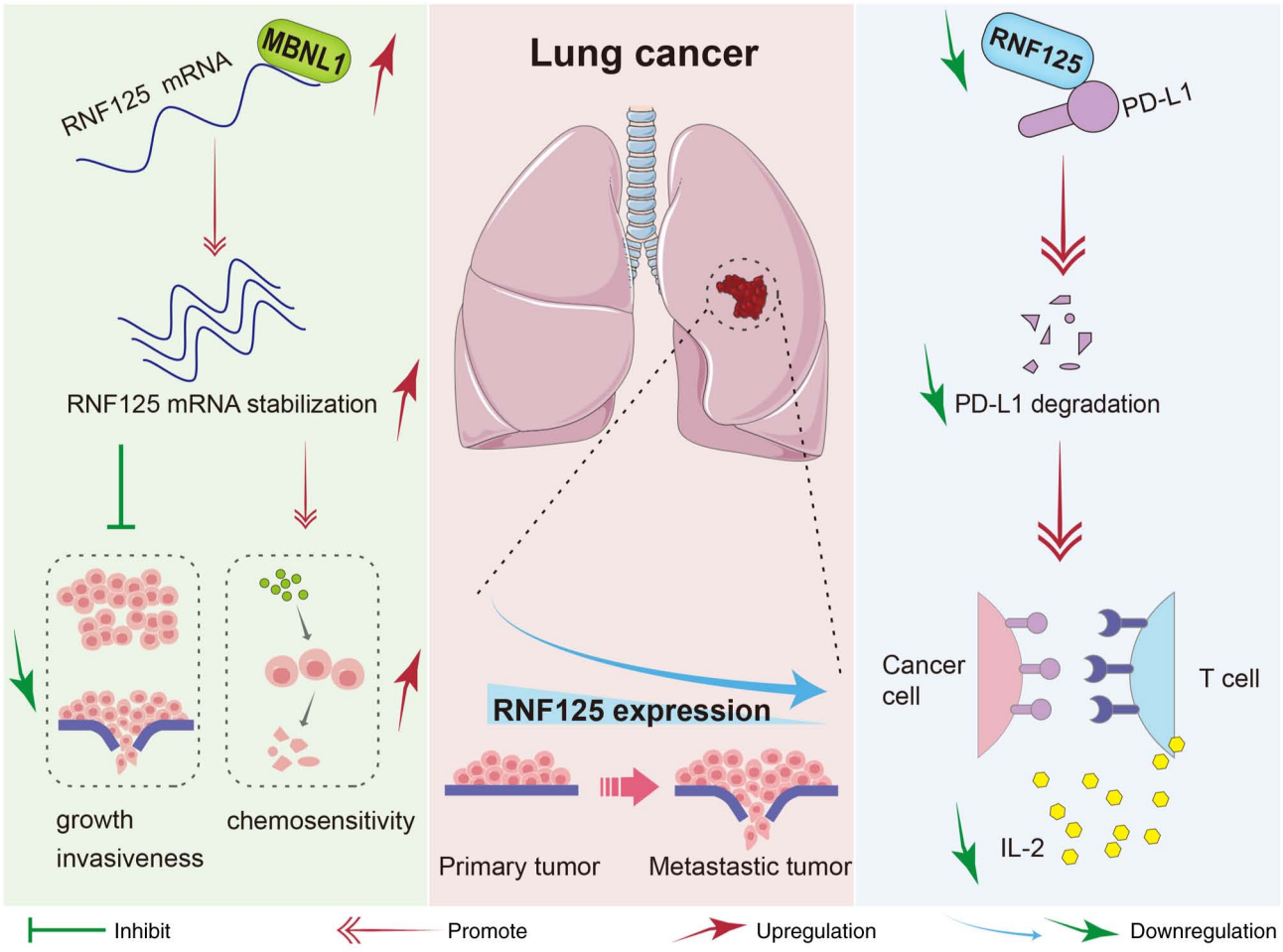

Figure 8. Schematic diagram of the function and molecular regulatory mechanism of RNF125 in LC. RNF125 is downregulated in lung cancer, and its low expression is associated with advanced-stage disease. RNF125 inhibits the LUAD cell growth and invasiveness and enhances the chemosensitivity of LUAD cells to cisplatin. RNF125 acts as an E3 ubiquitin ligase of PD-L1. Knockdown of RNF125 suppresses PD-L1 degradation, thereby impairing Tcell activation and antitumor cytokine secretion. Mechanistically, the RBP MBNL1 serves as an upstream regulator of RNF125 by stabilizing RNF125 mRNA. The figure contains elements from Servier Medical Art (https://smart.servier.com/) under a Creative Commons 3.0 license. MBNL1, muscleblind-like 1; RNF125, ring finger protein 125; PD-L1, programmed cell death 1 ligand 1; LUAD, lung adenocarcinoma.

The effect of MBNL1 on RNF125 expression in LUAD cells was examined. RT-qPCR and western blotting results suggested that the expression levels of MBNL1 and RNF125 were significantly upregulated upon MBNL1 overexpression and significantly downregulated upon MBNL1-silencing in LUAD cells (Fig. 7C and D). RIP-PCR demonstrated that MBNL1 protein bound to the 3'UTR of RNF125 transcripts (Fig. 7E). To verify the effect of MBNL1 on RNF125 transcript stability, LUAD cells were treated with the transcriptional inhibitor actinomycin D. Downregulation of MBNL1 promoted the decay of RNF125 mRNA, whereas overexpression of MBNL1 suppressed the decay of RNF125 mRNA, as demonstrated by qPCR assay (Fig. 7F and G). Additionally, MBNL1 overexpression suppressed the proliferation of LUAD cells compared with the empty vector control and RNF125 knockdown significantly eliminated the effect of MBNL1 overexpression compared with the corresponding control (Fig. 7H). Similarly, MBNL1 overexpression suppressed the invasion of LUAD cells and RNF125 knockdown eliminated the effect of MBNL1 overexpression compared with the corresponding control groups (Fig. 7I). Overall, these results suggested that MBNL1 may be an upstream regulator of RNF125 in LUAD.

Fig. 8 depicts a schematic diagram of the function and molecular regulatory mechanism of RNF125 in LC. In short, RNF125 is downregulated in LC, and its low expression is associated with advanced-stage disease. RNF125 inhibits the LUAD cell growth and invasiveness and enhances the chemosensitivity of LUAD cells to cisplatin. RNF125 acts as an E3 ubiquitin ligase of PD-L1. Knockdown of RNF125 suppresses PD-L1 degradation, thereby impairing T-cell activation and anti-tumor cytokine secretion. Mechanistically, the RBP MBNL1 serves as an upstream regulator of RNF125 by stabilizing RNF125 mRNA.

Discussion

Ubiquitin E3 ligases exert an important role in eukaryotes by facilitating protein ubiquitination and degradation (57). RNF125 is a ubiquitin E3 ligase that is aberrantly expressed in several cancers, including hepatocellular carcinoma, head and neck squamous cell carcinoma and melanoma, and has been

reported to inhibit tumor progression (12-15). However, its function in LUAD has not been reported. In the present study, the tumor suppressor role of RNF125 in LUAD was described and MBNL1 was proposed as a potential upstream regulator of RNF125 by controlling the stability of RNF125 mRNA.

Analysis based on clinical data showed that the RNF125 expression level was decreased and associated with metastatic status, advanced tumor stage and poor overall survival in LC, indicating a tumor suppressor role of RNF125 in LC. Kodama *et al* (11) reported that RNF125 limited hepatocellular carcinoma progression by inhibiting cancer cell proliferation. Consistent with the aforementioned results, the data from the present study showed that the overexpression of RNF125 inhibited LUAD cell growth. Moreover, it was demonstrated that RNF125 overexpression also inhibited cell migration and invasion. These findings suggested that RNF125 serves an important role in suppressing LUAD progression.

Platinum-based chemotherapy, particularly the use of cisplatin, is an important treatment for patients with advanced LUAD (7,58). Yet, the application of this drug is hampered by the poor response of patients with advanced LUAD to chemotherapy (59,60). Therefore, it is warranted to develop innovative and efficient strategies for increasing the sensitivity of LUAD cells to drug therapy. In the present study, it was demonstrated that knockdown of RNF125 decreased cisplatin-mediated cell apoptosis which corresponded with an increase in cell viability, whereas the overexpression of RNF125 exerted antithetical effects. In terms of molecular mechanisms, RNF125 knockdown reduced the activity of caspase-3 and the expression levels of cleaved PARP in cisplatin-treated LUAD cells. Similarly, downregulated RNF125 has been found to contribute to the resistance of melanoma to BRAF inhibitors (15). These findings support a potential role for RNF125 in regulating the sensitivity of tumor cells to therapeutic agents.

PD-L1 serves a critical role in regulating immune evasion, particularly in suppressing T cell functions (17,61-64). Previous research has shown that RNF125 suppresses immune escape by reducing PD-L1 expression through promoting PD-L1 ubiquitination and proteasomal degradation (14,20). In the present study, it was demonstrated that knockdown of RNF125 downregulated PD-L1 in LUAD cells and inhibited T cell activation. These findings suggest a potential link to RNF125-mediated modulation of PD-L1 with the previously reported role of RNF125 as a positive regulator of T cell activation (11). In addition, it was observed that the knockdown of RNF125 impaired NK cell lysis of LUAD cells. Taken together, these findings indicate that RNF125 may be an important regulator of immune evasion of LUAD. In addition, it was also hypothesized that the role of RNF125 in antitumor immunity might be associated with macrophages. As shown in the IHC staining of RNF125 in the Human Protein Atlas database (https://www.proteinatlas.org/ENSG00000101695-RNF125/tissue/lung) (31), medium expression of RNF125 in the normal lung was observed in macrophages, which requires further investigation into the specific function of RNF125 in macrophages and immune regulation.

RBP MBNL1 is a class of RNA metabolism regulators that control pre-mRNA splicing (65). Increasing MBNL1 protein expression levels in tumors inhibits tumor progression, resulting in notably prolonged survival of mice bearing human glioma stem cell-derived orthotopic xenografts (22). A previous study reported that MBNL1 increased the mRNA stability of metastasis suppressors debrin like (DBNL) and transforming acidic coiled-coil containing protein 1 (TACC1) to inhibit the invasiveness of breast cancer cells by binding to the 3'UTRs of DBNL and TACC1 mRNA (21). In the present study, the data showed that RNF125 knockdown abrogated the inhibitory effects of MBNL1 overexpression on proliferation and invasion of LUAD cells. Mechanistically, the MBNL1 protein bound to the 3'UTR of RNF125 transcripts and enhanced its stability, thereby promoting RNF125 expression. Correlation analysis demonstrated a positive correlation between the expression levels of RNF125 and MBNL1 in tumor tissues derived from patients with LUAD. These results indicated that MBNL1/RNF125 may serve an important role in regulating LUAD progression.

In summary, the present study demonstrated that RNF125 served a tumor suppressor role in LUAD. Moreover, MBNL1 augmented RNF125 expression levels through binding to the 3'UTR of RNF125 transcripts. Collectively, these findings provided potential novel therapeutic targets for LUAD treatment in the future.

Acknowledgments

Not applicable.

Funding

Not applicable.

Availability of data and materials

The data generated in the present study may be requested from the corresponding author.

Authors' contributions

YY and XJ were responsible for designing the methodology and performing experiments. YY and XK performed data analysis. XK visualized the data. JB curated the data. JB and BN were responsible for data validation. YY drafted the manuscript and SX reviewed and edited the manuscript. ZR contributed to the conceptualization and supervision of the project. JG contributed to data curation and project administration. SX conceptualized the study and provided resources. All authors read and approved the final version of the manuscript. YY and SX confirm the authenticity of all the raw data.

Ethics approval and consent to participate

LUAD samples and paired non-cancerous samples were obtained in accordance with the protocol approved by the Ethics Committee of Harbin Medical University Cancer Hospital approval no. JS2024-30; Harbin, China). Written informed consent to participate was obtained from each patient or the patient's guardian.

Patient consent for publication

Not applicable.

Competing interests

The authors declare that they have no competing interests.

References

1. Jones GS and Baldwin DR: Recent advances in the management of lung cancer. Clin Med (Lond) 18 (Suppl 2): S41-S46, 2018.
2. Nasim F, Sabath BF and Eapen GA: Lung cancer. Med Clin North Am 103: 463-473, 2019.
3. Bray F, Laversanne M, Sung H, Ferlay J, Siegel RL, Soerjomataram I and Jemal A: Global cancer statistics 2022: GLOBOCAN estimates of incidence and mortality worldwide for 36 cancers in 185 countries. CA Cancer J Clin 74: 229-263, 2024.
4. Denisenko TV, Budkevich IN and Zhivotovsky B: Cell death-based treatment of lung adenocarcinoma. Cell Death Dis 9: 117, 2018.
5. Kuhn E, Morbini P, Cancellieri A, Damiani S, Cavazza A and Comin CE: Adenocarcinoma classification: Patterns and prognosis. Pathologica 110: 5-11, 2018.
6. Nguyen TT, Lee HS, Burt BM, Wu J, Zhang J, Amos CI and Cheng C: A lepidic gene signature predicts patient prognosis and sensitivity to immunotherapy in lung adenocarcinoma. Genome Med 14: 5, 2022.
7. Nooreldeen R and Bach H: Current and future development in lung cancer diagnosis. Int J Mol Sci 22: 8661, 2021.
8. Lahiri A, Maji A, Potdar PD, Singh N, Parikh P, Bisht B, Mukherjee A and Paul MK: Lung cancer immunotherapy: Progress, pitfalls, and promises. Mol Cancer 22: 40, 2023.
9. Glickman MH and Ciechanover A: The ubiquitin-proteasome proteolytic pathway: Destruction for the sake of construction. Physiol Rev 82: 373-428, 2002.
10. Zhao H, Li CC, Pardo J, Chu PC, Liao CX, Huang J, Dong JG, Zhou X, Huang Q, Huang B, *et al*: A novel E3 ubiquitin ligase TRAC-1 positively regulates T cell activation. J Immunol 174: 5288-5297, 2005.
11. Giannini AL, Gao Y and Bijlmakers MJ: T-cell regulator RNF125/TRAC-1 belongs to a novel family of ubiquitin ligases with zinc fingers and a ubiquitin-binding domain. Biochem J 410: 101-111, 2008.
12. Kodama T, Kodama M, Jenkins NA, Copeland NG, Chen HJ and Wei Z: Ring finger protein 125 is an anti-proliferative tumor suppressor in hepatocellular carcinoma. Cancers (Basel) 14: 2589, 2022.
13. Feng Z, Ke S, Wang C, Lu S, Xu Y, Yu H, Li Z, Yin B, Li X, Hua Y, *et al*: RNF125 attenuates hepatocellular carcinoma progression by downregulating SRSF1-ERK pathway. Oncogene 42: 2017-2030, 2023.
14. Jiang C, He L, Xiao S, Wu W, Zhao Q and Liu F: E3 ubiquitin ligase RNF125 suppresses immune escape in head and neck squamous cell carcinoma by regulating PD-L1 expression. Mol Biotechnol 65: 891-903, 2023.
15. Kim H, Frederick DT, Levesque MP, Cooper ZA, Feng Y, Krepler C, Brill L, Samuels Y, Hayward NK, Perlina A, *et al*: Downregulation of the ubiquitin ligase RNF125 underlies resistance of melanoma cells to BRAF inhibitors via JAK1 deregulation. Cell Rep 11: 1458-1473, 2015.
16. Han Y, Liu D and Li L: PD-1/PD-L1 pathway: Current researches in cancer. Am J Cancer Res 10: 727-742, 2020
17. Cha JH, Chan LC, Li CW, Hsu JL and Hung MC: Mechanisms controlling PD-L1 expression in cancer. Mol Cell 76: 359-370, 2019.
18. Chen W, Saxton B, Tessema M and Belinsky SA: Inhibition of GFAT1 in lung cancer cells destabilizes PD-L1 protein. Carcinogenesis 42: 1171-1178, 2021.
19. Ma J, Chi D, Wang Y, Yan Y, Zhao S, Liu H, Jing J, Pu H and Zhang M: Prognostic value of PD-L1 expression in resected lung adenocarcinoma and potential molecular mechanisms. J Cancer 9: 3489-3499, 2018.
20. Wei M, Mo Y, Liu J, Zhai J, Li H, Xu Y, Peng Y, Tang Z, Wei T, Yang X, *et al*: Ubiquitin ligase RNF125 targets PD-L1 for ubiquitination and degradation. Front Oncol 12: 835603, 2022.
21. Fish L, Pencheva N, Goodarzi H, Tran H, Yoshida M and Tavazoie SF: Muscleblind-like 1 suppresses breast cancer metastatic colonization and stabilizes metastasis suppressor transcripts. Genes Dev 30: 386-398, 2016.
22. Zhang Q, Wu Y, Chen J, Tan F, Mou J, Du Z, Cai Y, Wang B and Yuan C: The regulatory role of both MBNL1 and MBNL1-AS1 in several common cancers. Curr Pharm Des 28: 581-585, 2022.
23. Ray D, Yun YC, Idris M, Cheng S, Boot A, Iain TBH, Rozen SG, Tan P and Epstein DM: A tumor-associated splice-isoform of MAP2K7 drives dedifferentiation in MBNL1-low cancers via JNK activation. Proc Natl Acad Sci USA 117: 16391-16400, 2020.
24. Voss DM, Sloan A, Spina R, Ames HM and Bar EE: The alternative splicing factor, MBNL1, inhibits glioblastoma tumor initiation and progression by reducing hypoxia-induced stemness. Cancer Res 80: 4681-4692, 2020.
25. Li T, Fu J, Zeng Z, Cohen D, Li J, Chen Q, Li B and Liu XS: TIMER2.0 for analysis of tumor-infiltrating immune cells. Nucleic Acids Res 48(W1): W509-W514, 2020.
26. Cook KB, Kazan H, Zuberi K, Morris Q and Hughes TR: RBPDB: A database of RNA-binding specificities. Nucleic Acids Res 39: D301-D308, 2011.
27. Girard L, Rodriguez-Canales J, Behrens C, Thompson DM, Botros IW, Tang H, Xie Y, Rekhtman N, Travis WD, Wistuba II, *et al*: An expression signature as an aid to the histologic classification of non-small cell lung cancer. Clin Cancer Res 22: 4880-4889, 2016.
28. Okayama H, Kohno T, Ishii Y, Shimada Y, Shiraishi K, Iwakawa R, Furuta K, Tsuta K, Shibata T, Yamamoto S, *et al*: Identification of genes upregulated in ALK-positive and EGFR/KRAS/ALK-negative lung adenocarcinomas. Cancer Res 72: 100-111, 2012.
29. Yamauchi M, Yamaguchi R, Nakata A, Kohno T, Nagasaki M, Shimamura T, Imoto S, Saito A, Ueno K, Hatanaka Y, *et al*: Epidermal growth factor receptor tyrosine kinase defines critical prognostic genes of stage I lung adenocarcinoma. PLoS One 7: e43923, 2012.
30. Leon LM, Gautier M, Allan R, Ilié M, Nottet N, Pons N, Paquet A, Lebrigand K, Truchi M, Fassy J, *et al*: The nuclear hypoxia-regulated NLUCAT1 long non-coding RNA contributes to an aggressive phenotype in lung adenocarcinoma through regulation of oxidative stress. Oncogene 38: 7146-7165, 2019.
31. Pontén F, Jirström K and Uhlen M: The human protein atlas-a tool for pathology. J Pathol 216: 387-393, 2008.
32. Bartha Á and Győrffy B: TNMplot.com: A web tool for the comparison of gene expression in normal, tumor and metastatic tissues. Int J Mol Sci 22: 2622, 2021.
33. Ru B, Wong CN, Tong Y, Zhong JY, Zhong SSW, Wu WC, Chu KC, Wong CY, Lau CY, Chen I, *et al*: TISIDB: An integrated repository portal for tumor-immune system interactions. Bioinformatics 35: 4200-4202, 2019.
34. Rousseaux S, Debernardi A, Jacquiau B, Vitte AL, Vesin A, Nagy-Mignotte H, Moro-Sibilot D, Brichon PY, Lantuejoul S, Hainaut P, *et al*: Ectopic activation of germline and placental genes identifies aggressive metastasis-prone lung cancers. Sci Transl Med 5: 186ra66, 2013.
35. Takeuchi T, Tomida S, Yatabe Y, Kosaka T, Osada H, Yanagisawa K, Mitsudomi T and Takahashi T: Expression profile-defined classification of lung adenocarcinoma shows close relationship with underlying major genetic changes and clinicopathologic behaviors. J Clin Oncol 24: 1679-1688, 2006.
36. Matsuyama Y, Suzuki M, Arima C, Huang QM, Tomida S, Takeuchi T, Sugiyama R, Itoh Y, Yatabe Y, Goto H and Takahashi T: Proteasomal non-catalytic subunit PSMD2 as a potential therapeutic target in association with various clinicopathologic features in lung adenocarcinomas. Mol Carcinog 50: 301-309, 2011.
37. Goswami CP and Nakshatri H: PROGgeneV2: Enhancements on the existing database. BMC Cancer 14: 970, 2014.
38. Stark C, Breitkreutz BJ, Reguly T, Boucher L, Breitkreutz A and Tyers M: BioGRID: A general repository for interaction datasets. Nucleic Acids Res 34 (Database issue): D535-D539, 2006.
39. Warde-Farley D, Donaldson SL, Comes O, Zuberi K, Badrawi R, Chao P, Franz M, Grouios C, Kazi F, Lopes CT, *et al*: The GeneMANIA prediction server: Biological network integration for gene prioritization and predicting gene function. Nucleic Acids Res 38 (Web Server issue): W214-W220, 2010.
40. Sherman BT, Hao M, Qiu J, Jiao X, Baseler MW, Lane HC, Imamichi T and Chang W: DAVID: A web server for functional enrichment analysis and functional annotation of gene lists (2021 update). Nucleic Acids Res 50(W1): W216-W221, 2022.

41. Stelzer G, Rosen N, Plaschkes I, Zimmerman S, Twik M, Fishilevich S, Stein TI, Nudel R, Lieder I, Mazor Y, *et al*: The GeneCards suite: From gene data mining to disease genome sequence analyses. Curr Protoc Bioinformatics 54: 1.30.1-1.30.33, 2016.
42. Paz I, Kosti I, Ares M Jr, Cline M and Mandel-Gutfreund Y: RBPmap: A web server for mapping binding sites of RNA-binding proteins. Nucleic Acids Res 42: W361-W367, 2014.
43. Li Z, Chen S, Jhong JH, Pang Y, Huang KY, Li S and Lee TY: UbiNet 2.0: A verified, classified, annotated and updated database of E3 ubiquitin ligase-substrate interactions. Database (Oxford) 8: baab010, 2021.
44. Livak KJ and Schmittgen TD: Analysis of relative gene expression data using real-time quantitative PCR and the 2(-Delta Delta C(T)) method. Methods 25: 402-408, 2001.
45. Amin EM, Liu Y, Deng S, Tan KS, Chudgar N, Mayo MW, Sanchez-Vega F, Adusumilli PS, Schultz N and Jones DR: The RNA-editing enzyme ADAR promotes lung adenocarcinoma migration and invasion by stabilizing FAK. Sci Signal 10: eaah3941, 2017.
46. Siang DTC, Lim YC, Kyaw AMM, Win KN, Chia SY, Degirmenci U, Hu X, Tan BC, Walet ACE, Sun L and Xu D: The RNA-binding protein HuR is a negative regulator in adipogenesis. Nat Commun 11: 213, 2020.
47. Jia Y, Vong JS, Asafova A, Garvalov BK, Caputo L, Cordero J, Singh A, Boettger T, Günther S, Fink L, *et al*: Lamin B1 loss promotes lung cancer development and metastasis by epigenetic derepression of RET. J Exp Med 216: 1377-1395, 2019.
48. Kostyrko K, Román M, Lee AG, Simpson DR, Dinh PT, Leung SG, Marini KD, Kelly MR, Broyde J, Califano A, *et al*: UHRF1 is a mediator of KRAS driven oncogenesis in lung adenocarcinoma. Nat Commun 14: 3966, 2023.
49. Hong SY, Kao YR, Lee TC and Wu CW: Upregulation of E3 ubiquitin ligase CBLC enhances EGFR dysregulation and signaling in lung adenocarcinoma. Cancer Res 78: 4984-4996, 2018.
50. Volonte D, Sedorovitz M and Galbiati F: Impaired Cdc20 signaling promotes senescence in normal cells and apoptosis in non-small cell lung cancer cells. J Biol Chem 298: 102405, 2022.
51. Cai S, Zhang B, Huang C, Deng Y, Wang C, Yang Y, Xiang Z, Ni Y, Wang Z, Wang L, *et al*: CTRP6 protects against ferroptosis to drive lung cancer progression and metastasis by destabilizing SOCS2 and augmenting the xCT/GPX4 pathway. Cancer Lett 579: 216465, 2023.
52. Zhang S, You X, Zheng Y, Shen Y, Xiong X and Sun Y: The UBE2C/CDH1/DEPTOR axis is an oncogene and tumor suppressor cascade in lung cancer cells. J Clin Invest 133: e162434, 2023.
53. Hua TNM, Namkung J, Phan ANH, Vo VTA, Kim MK, Jeong Y and Choi JW: PPARgamma-mediated ALDH1A3 suppression exerts anti-proliferative effects in lung cancer by inducing lipid peroxidation. J Recept Signal Transduct Res 38: 191-197, 2018.
54. Wu J, Wen T, Marzio A, Song D, Chen S, Yang C, Zhao F, Zhang B, Zhao G, Ferri A, *et al*: FBXO32-mediated degradation of PTEN promotes lung adenocarcinoma progression. Cell Death Dis 15: 282, 2024.
55. Kildey K, Gandhi NS, Sahin KB, Shah ET, Boittier E, Duijf PHG, Molloy C, Burgess JT, Beard S, Bolderson E, *et al*: Elevating CDCA3 levels in non-small cell lung cancer enhances sensitivity to platinum-based chemotherapy. Commun Biol 4: 638, 2021.
56. Zhang R, Zhang W, Zeng Y, Li Y, Zhou J, Zhang Y, Wang A, Lv Y, Zhu J, Liu Z and Huang JA: The regulation of CPNE1 ubiquitination by the NEDD4L is involved in the pathogenesis of non-small cell lung cancer. Cell Death Discov 7: 336, 2021.
57. Zheng N and Shabek N: Ubiquitin ligases: Structure, function, and regulation. Annu Rev Biochem 86: 129-157, 2017.
58. Konoshenko M, Lansukhay Y, Krasilnikov S and Laktionov P: MicroRNAs as predictors of lung-cancer resistance and sensitivity to cisplatin. Int J Mol Sci 23: 7594, 2022.
59. Taheri M, Shoorei H, Anamag FT, Ghafouri-Fard S and Dinger ME: LncRNAs and miRNAs participate in determination of sensitivity of cancer cells to cisplatin. Exp Mol Pathol 123: 104602, 2021.
60. Lv P, Man S, Xie L, Ma L and Gao W: Pathogenesis and therapeutic strategy in platinum resistance lung cancer. Biochim Biophys Acta Rev Cancer 1876: 188577, 2021.
61. Gou Q, Dong C, Xu H, Khan B, Jin J, Liu Q, Shi J and Hou Y: PD-L1 degradation pathway and immunotherapy for cancer. Cell Death Dis 11: 955, 2020.
62. Xiong W, Gao Y, Wei W and Zhang J: Extracellular and nuclear PD-L1 in modulating cancer immunotherapy. Trends Cancer 7: 837-846, 2021.
63. Sun C, Mezzadra R and Schumacher TN: Regulation and function of the PD-L1 checkpoint. Immunity 48: 434-452, 2018.
64. Yu H, Boyle TA, Zhou C, Rimm DL and Hirsch FR: PD-L1 expression in lung cancer. J Thorac Oncol 11: 964-975, 2016.
65. Hung CS and Lin JC: Alternatively spliced MBNL1 isoforms exhibit differential influence on enhancing brown adipogenesis. Biochim Biophys Acta Gene Regul Mech 1863: 194437, 2020.